



HAL
open science

Visual servo system based on a biologically inspired scanning sensor

Stephane Viollet, Nicolas Franceschini

► **To cite this version:**

Stephane Viollet, Nicolas Franceschini. Visual servo system based on a biologically inspired scanning sensor. Photonics East '99, Aug 1999, Boston, France. pp.144-155, 10.1117/12.360334 . hal-03844361

HAL Id: hal-03844361

<https://amu.hal.science/hal-03844361>

Submitted on 8 Nov 2022

HAL is a multi-disciplinary open access archive for the deposit and dissemination of scientific research documents, whether they are published or not. The documents may come from teaching and research institutions in France or abroad, or from public or private research centers.

L'archive ouverte pluridisciplinaire **HAL**, est destinée au dépôt et à la diffusion de documents scientifiques de niveau recherche, publiés ou non, émanant des établissements d'enseignement et de recherche français ou étrangers, des laboratoires publics ou privés.

Visual servo system based on a biologically-inspired scanning sensor

Stéphane Viollet*, Nicolas Franceschini**

C.N.R.S, Laboratoire de Neurobiologie, LNB3
31, chemin Joseph Aiguier
13402 Marseille Cedex 20, FRANCE

ABSTRACT

In the framework of our biologically inspired robotics approach, we describe a visually-guided demonstration model aircraft, the attitude of which is stabilized in yaw by means of a novel, non emissive optical sensor having a small visual field. This aircraft incorporates a miniature scanning sensor consisting of two photoreceptors with adjacent visual axes, driving a Local Motion Detector (LMD), which are made to perform a low-amplitude scanning at a varying angular speed. Under these conditions, the signal output from the motion detector varies gradually with the angular position of a contrasting object placed in its visual field, actually making the complete system a non-emissive optical "position sensor". Its output, remarkably, (i) varies quasi-linearly with the angular position of the contrasting object, and (ii) remains largely invariant with respect to the distance to the object and its degree of contrast.

We built a miniature, twin-engine, twin-propeller aircraft (weight 100 grammes) equipped with this visual position sensor. After incorporating the sensor into a visuomotor feedback loop enhanced by an inertial sensor, we established that the "sighted aircraft" can fixate and track a dark edge placed in its visual field, thus opening the way for the development of visually-guided systems for controlling the attitude of micro-air vehicles, of the kind observed in insects such as hover-flies.

Keywords : vision, optical sensor, position sensor, non-emissive sensor, scanning, tracking, visual fixation, motion detection, micro air vehicles, attitude control.

1. INTRODUCTION

The present study was carried out in the context of our previous studies using a biologically-inspired minimalistic robotic approach, which were based on the idea of reconstructing natural visuomotor processes in order to better understand them.¹⁻⁵ Here we show that an elementary visual sensor composed of only two pixels is able to accurately detect contrasting features within its visual field, provided it uses a particular scanning mode, such as that recently discovered in the compound eye of flies.⁶ This low-cost, low-weight, low-complexity scanning sensor was found to deliver an output which is:

- quasi-linear with respect to the angular position of a contrasting object in its field of view.
- largely invariant with respect to the distance to the object and its level of contrast.

The most novel feature of this visual sensor, which differs from other systems based on *scanning at constant angular speed*⁴ and *pulse-scanning*,⁷ is that it scans the visual field at an angular speed which varies gradually with time (*variable speed scanning*). The sensor's output then becomes a graded function of the position of a contrast feature within its visual field, with the interesting consequence that if this sensor is incorporated into a visuomotor control loop, it is able to stabilize a robot such as a micro air-vehicle with respect to the environmental features.

In sections 2 and 3, we simulate the pure rotation at a variable speed of a pair of pixels in front of a stationary contrast feature (a light-to-dark edge) and show that the processing of the apparent motion yields a signal which gradually varies with the angular position of the edge in the visual field. In section 4, we describe the structure of a miniature scanning sensor coupled with a Local Motion Detector (LMD) based on the fly compound eye.⁸ In section 5, we describe the structure of a miniature twin-engine propeller aircraft equipped with the scanning sensor, and the implementation of a visual feedback loop designed to stabilize this model aircraft in yaw. The scanning sensor picks up an error signal, which is used to drive the two propellers differentially, causing the "seeing aircraft" to reorient and adjust its line of sight so as to remain constantly locked onto a nearby or distant contrasting target.

* Email: sviollet@lnb.cnrs-mrs.fr; Fax : 33.4.91.22.08.75 [In Proc Sensor Fusion and Decentralized Control in Robotics Systems II Conf.](#)

** enfranceschini@lnb.cnrs-mrs.fr; Fax : 33.4.91.22.08.75 [SPIE, Boston, Vol. 3839, pp. 144-155, September 1999.](#)

Contrary to the kind of yaw stabilization which can be achieved with a gyroscope having similar low-weight and low-cost characteristics, that described here is not only stiff but also devoid of drift. Some examples are given below, where the (tethered) aircraft either tracks a slowly moving dark edge or maintains fixation onto a stationary target for 17 minutes.

The scanning visual sensor and the visuomotor control loop we have developed are appropriate for:

- detecting low speed relative motion between a craft and its environment.
- rejecting environmental disturbances by maintaining visual fixation onto a nearby or distant target, regardless of its contrast and distance within a given range.
- and controlling the attitude of a craft optically with respect to environmental features.

2. SCANNING AT A VARIABLE ANGULAR SPEED

2.1. Photoreceptor model

The angular sensitivity of an insect lens-photoreceptor combination is usually approximated by a bell-shaped function.⁹ In the present case, we use a Gaussian function, the bottom part of which is truncated below the threshold s_0 .

The angular sensitivity $S(\varphi)$ of a photosensor i is therefore given by:

$$S(\varphi) = \left(\frac{\text{abs}(G_i(\varphi) - s_0) + (G_i(\varphi) - s_0)}{2} \right), \quad (1)$$

$$\text{with } G_i(\varphi) = \exp \left[-\frac{\varphi^2}{2\sigma^2} \right] \quad (2)$$

The main parameters which characterize $S(\varphi)$ are as follows :

- L_v : total angular width of the visual field
- $\Delta\rho$: angular width at half height

Both parameters can be expressed with respect to σ as follows:

$$\Delta\rho = 2\sigma \left[2 \ln \left(\frac{2}{1 + s_0} \right) \right]^{\frac{1}{2}} \quad (3)$$

$$L_v = 2\sigma \left[2 \ln \left(\frac{1}{s_0} \right) \right]^{\frac{1}{2}} \quad (4)$$

2.2. Variable angular speed

As sketched in Figure 1a, we have simulated the concerted rotation of two photosensors, 1 and 2, separated by a constant angle $\Delta\varphi$, called the interreceptor angle, in front of an elementary panorama consisting of a single segment AB. The pair of photosensors is assumed here to rotate clockwise at an angular speed Ω which decays exponentially with time. The angle ψ is given by (Fig 1b):

$$\psi(t) = A \left(1 - \exp \left(-\frac{t}{\tau} \right) \right) \quad (5)$$

Hence the angular speed $\Omega(t)$ is:

$$\Omega(t) = \frac{A}{\tau} \exp \left(-\frac{t}{\tau} \right) \quad (6)$$

The position of the segment is defined by the points $A(x_1, y_1)$ and $B(x_2, y_2)$ with $y_1 = y_2$.

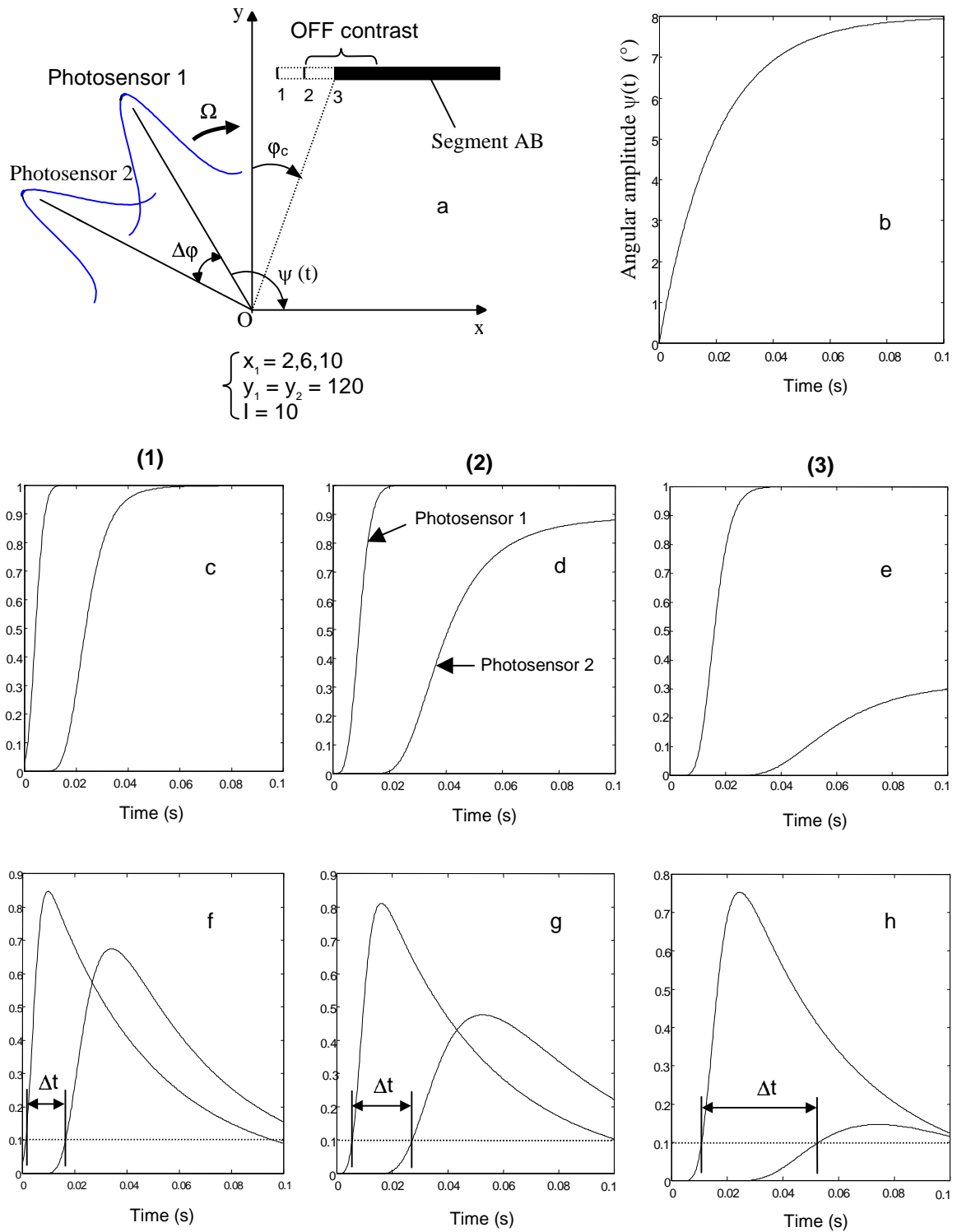


Fig. 1 Simulated response of two adjacent photosensors rotating clockwise at a variable angular speed Ω , and encountering a dark edge placed at various positions 1, 2, 3 (a).

(b) variation of angle $\psi(t)$.

(c, d, e) output from photosensors 1 and 2, depending of the position of the dark edge (1,2,3).

(f, g, h) high-pass filtered version of (c,d,e) (cutt-off frequency : 2Hz) and thresholding of the output signal from each photosensor.

$\Delta\rho = 2^\circ$, $\Delta\phi = 4^\circ$, $Lv = 5.2^\circ$, $\xi = 0.01$, $A = 2\Delta\phi$, $\tau = 20\text{ms}$, $T = 0.01\text{s}$

At any time, the output $R_i(t)$ from photosensor i is obtained by integrating the angular sensitivity $S(\varphi)$ weighted by the intensity $I(\varphi)$:

$$R_i(t) = \int_{-L_v/2}^{L_v/2} I(\varphi)S(\varphi)d\varphi \quad (7)$$

2.3. Processing the photoreceptor signals

To calculate the output signal from each photoreceptor, we used a discrete version of equation (7). The signal sampled, $R_i(kT)$, with T in seconds, results from a convolution of the light intensity I with the Gaussian mask $S(kTs)$ (Ts in degrees). In other words, at each value of ψ , $R_i(kT)$ results from the filtering of I by a filter with a Gaussian-shaped impulse response. In all these calculations, the Gaussian mask $S(kTs)$ based on equation (1) was processed with a spatial sampling step Ts equal to 0.004° . $R_i(kT)$ was normalized with respect to its extremal values:

- $R_i(kT) = 1$ when a black segment ($I = 10$) covers the whole visual field L_v .
- $R_i(kT) = 0$ when the black segment is completely outside the visual field ($I = 0$).

In order to show that the time lag between the two photosensors varies with the *position* of the contrast feature, we refer to the scheme of Figure 1a, in which we put the dark edge at 3 positions (1,2,3) along the x axis. For each of these stationary positions, Figures 1(c,d,e) give the output from photosensors 1 and 2 as they turn clockwise at a variable angular speed Ω . In Figures 1(f,g,h), the output from each photosensor was passed through an analog high-pass filter with a cut-off frequency of 2Hz.

Fig 1(f,g,h) shows that the time lag Δt between the differentiated and thresholded outputs of the two photosensors indeed varies gradually with the angular position φ_c of the contrast edge within the visual field.

3. MEASURING ANGULAR SPEED WITH AN LMD

The Local Motion Detector (LMD) - also called the Elementary Motion Detector (EMD) - is an analog circuit yielding an output signal which decreases gradually when the time lag Δt between its two inputs increases (cf section 1.3). Like many insect motion detecting neurons,⁸ the analog LMD is directionally selective. We designed an LMD which detects only light-to-dark transitions ("OFF contrasts") when the scanning direction is clockwise. The use of the derivative in the first LMD processing step is essential, as it makes it possible to :

- eliminate the DC level of the photosensors
- discriminate between positive (ON) contrasts and negative (OFF) contrasts.

A block diagram of the LMD is shown in Figure 2.

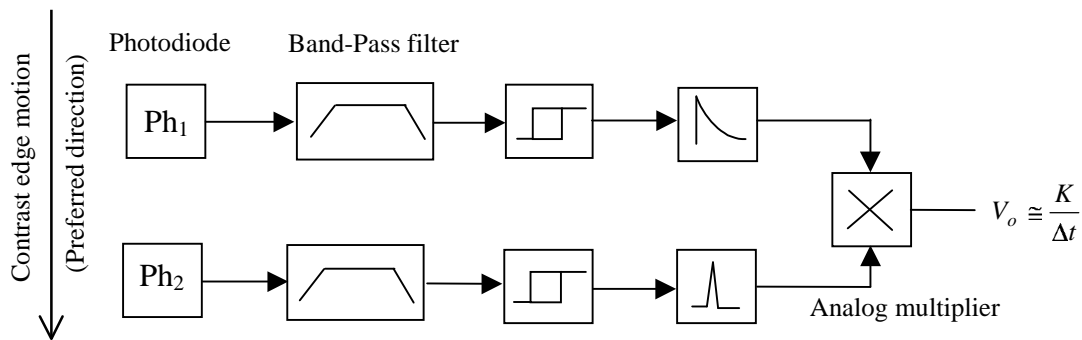


Fig. 2 Structure of the LMD

The signal output V_o results from multiplying an exponentially decaying pulse by a delayed fast pulse. V_o varies inversely with Δt and hence grows larger with Ω . This pulse-based scheme for an analog motion detector was originally designed¹⁰

on the basis of electrophysiological findings obtained at our laboratory on flies,⁸ and an array of motion detectors of this kind has been previously used onboard a visually guided autonomous robot capable of avoiding obstacles at 50cm/s.^{1,2}

It was predicted from the simulations shown in Figure 1, that if an LMD is driven by a pair of photosensors rotating at a variable angular speed, its output V_o will vary gradually with the angular position ϕ_c of a dark edge in the visual field of the scanning sensor.

4. VARIABLE SPEED SCANNING AND VISUAL POSITION SENSING

4.1. The scanning sensor

We built a miniature scanner, the components of which are sketched in Figure 3. A dual photosensor and a lens (focal length: 8mm), mounted opposite each other on a blackened perspex drum (diameter 15mm), form a miniature "camera eye", which is driven by a DC micromotor (diameter 10mm). The angle of divergence $\Delta\phi$ between the visual axes of the two photoreceptors ("interreceptor angle") is:

$$\Delta\phi = 4^\circ$$

The angular position of the drum (and hence, that of the sensor's line of sight) is monitored by a *magneto-resistive sensor* responding to the angular position of a micromagnet glued to the hub of the drum. This sensor is part of the loop of an accessory position-servo, which controls the eye so that it will follow any imposed signal.

This servo-eye is positioned by a composite periodic signal at 10 Hz (cf Figure 4a), which eventually leads to two scanning phases (cf Figure 4c):

1/ during the first phase (duration: 25ms), the angular speed Ω of the eye is made to decrease quasi-exponentially with time.

2/ during the longer "return phase" (duration 75 ms), the eye is made to return to its original position at a quasi-constant speed.

The amplitude $\Delta\xi$ of the scan is expressed in terms of the interreceptor angle $\Delta\phi$ by means of the scanning factor⁴ α :

$$\alpha = \frac{\Delta\xi}{\Delta\phi}$$

The LMD responds only during the first part of the scan (short phase), delivering an output which varies in a graded manner with the position of the contrasting edge within its visual field. Imposing a slow and constant angular speed during the return phase improves the robustness of the sensor, making it responsive to environmental features far beyond the simple edge considered here.

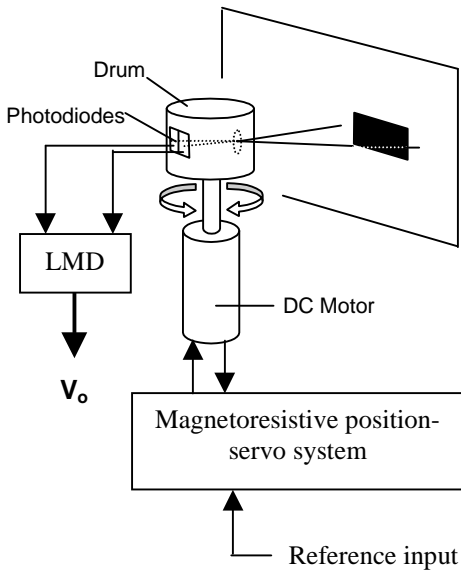


Fig. 3 Sketch of the complete visual scanning sensor in front of a dark object posted up on the wall.

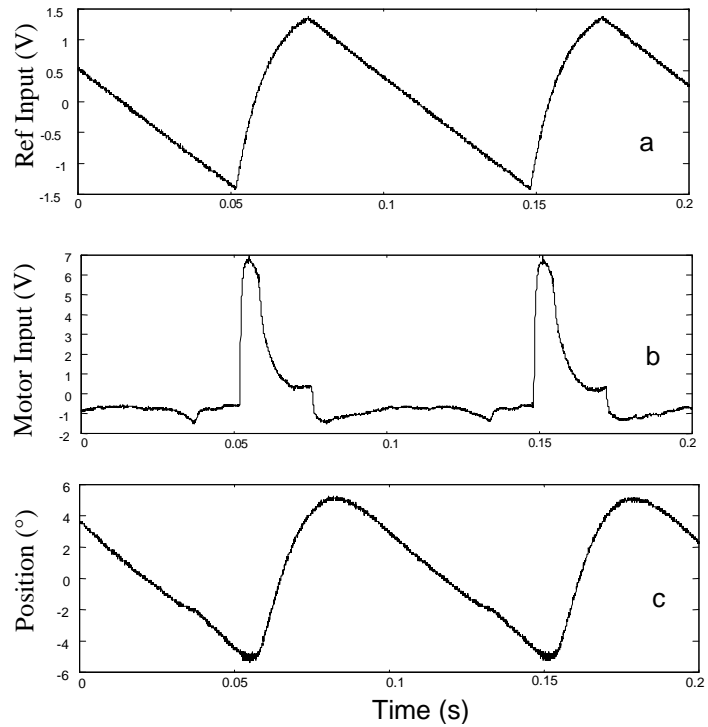


Fig. 4 Measured periodic signals from the position servo of the scanning eye. (a) reference input voltage imposed upon the position servo. (b) actual motor input voltage. (c) resulting orientation of the "eye" as monitored by the magneto-resistive sensor

4.2. Sensor output versus contrast and distance

The complete scanning sensor was mounted vertically onto the shaft of a resolver and a 16 bit resolver-to-digital converter was used to accurately determine the angular orientation of the sensor. The two photoreceptor outputs were connected to an LMD via soft microwires. We varied the orientation of the scanning sensor manually and at each orientation recorded the voltage output V_o from the LMD and the angular position φ_c of the sensor.

The object was a contrast step made of grey paper that stood out from the background. The contrast m was determined by measuring the relative illuminance of the paper (I_1) and its background (I_2) and calculating:

$$m = \frac{I_1 - I_2}{I_1 + I_2}$$

Contrast was measured *in situ* with a linear photo device having the same spectral sensitivity as the dual photosensor used.

Figures 5(a,b,c) show that the sensor output varies with the position of a contrasting edge within its visual field - as predicted, based on the results of Sections 1 and 3. The responses are quasi-linear with respect to the yaw orientation of the scanning sensor and largely invariant with respect to the contrast m and the distance D of the dark edge.⁵ Subtracting a reference signal $r = 5.5V$ from all the data gives an odd function, which is a useful feature for incorporating the scanning sensor into an optomotor loop. Moreover, invariance with respect to the distance - within a limited range - is an important feature for the dynamics of an optomotor loop of this kind, because it does not introduce any gain variations liable to cause instability.¹¹ The sensor was designed to be robust against any spurious modulations caused by neon room illumination (100Hz intensity modulations).

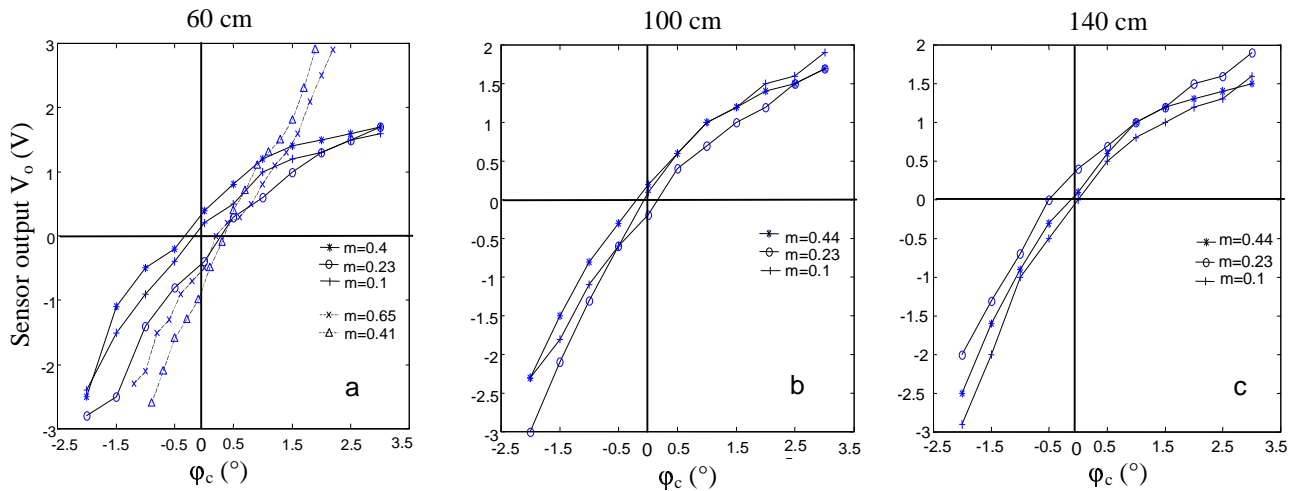


Fig. 5 Voltage output V_o from the scanning sensor (cf Fig 3) as a function of its orientation φ_c and the contrast m of the pattern. Accuracy: $\pm 50\text{mV}$.
 (a) response at $D = 60\text{cm}$ with respect to a dark edge (solid) and a dark stripe 10mm in width (dotted).
 (b) response at $D = 100\text{cm}$ to a dark edge of various contrasts.
 (c) response at $D = 140\text{cm}$ to the same dark edges.
 ($\Delta\varphi = 4^\circ, \alpha = 2$).

5. VISUAL CONTROL OF A MINIATURE TWIN-PROPELLER AIRCRAFT

A sketch of the tethered model aircraft equipped with its scanning sensor is shown in Figure 6.

This aircraft is made of carbon, wood, fiberglass, and EPS. Its total weight is 100g, including the engines, scanning sensor, gyroscope, and the complete electronics. The onboard battery (metal-hydride 7.2V-0.6A.h) weighs another 90g. In order to minimize the inertia around the yaw axis, the DC engines are positioned close to the axis of rotation and transmit their power to their respective propellers (diameter 13cm) via a 12 cm long carbon fiber shaft and bevel gear (reduction ratio 1/5). The SMD electronic components occupy five decks of printed circuit boards interconnected via miniature bus connectors, each board (diameter 55mm) being dedicated to a particular task, as follows:

- Board 1 : power conditioning
- Board 2 : RC receiver and PWM signal generator
- Board 3 : LMD
- Board 4 : optomotor controller
- Board 5 : scanner servo system

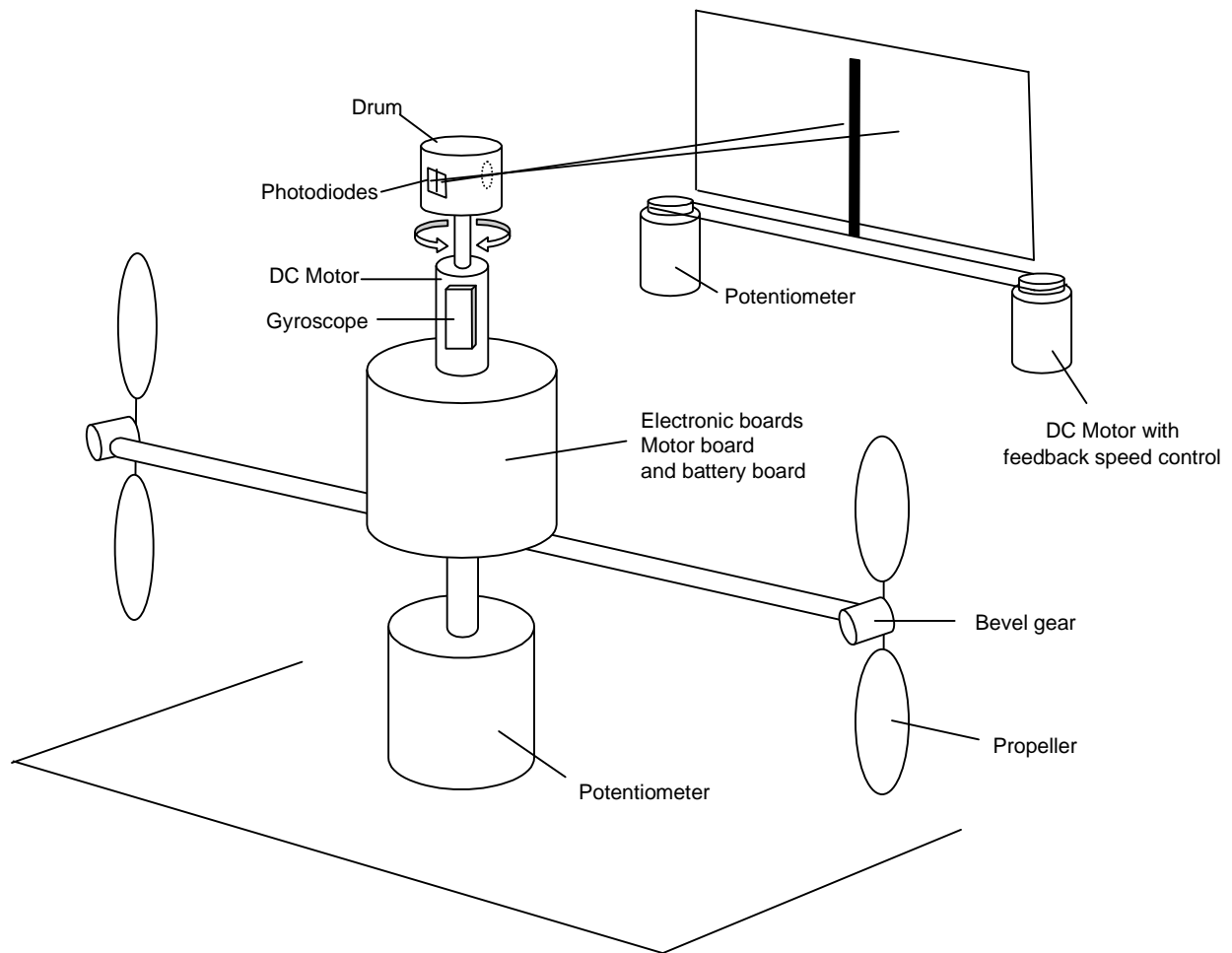


Fig. 6 Model aircraft equipped with its scanning sensor

5.1. Dynamic modelling of the twin-propeller aircraft

We analysed the dynamics of the twin-propeller system around its yaw axis from its response to a step input. In order to convey a step input voltage to the autonomous plant, we designed a remote control system operating at 433MHz (1000 baud). At the transmitter, the throttle and yaw commands were adjusted by means of "digital" joysticks. Onboard the aircraft, these signals were received by a miniature receiver and dispatched to two digital potentiometers via a PIC16F84 microcontroller. These potentiometers (8-bit digital-to-analog converters) generated a differential signal u_d to adjust the yaw and a signal u_c to adjust the common throttle. In order to make sure that the two thrusters reached the same nominal speed (i.e., the same "operating point") during each experimental run, the DC level u_c was memorized in the microcontroller flash memory and called back via a third remote control channel. The differential propeller driving system is shown in Figure 7.

The whole aircraft was fixed onto the shaft of the resolver (cf Section 4.1), which was selected because of its negligible friction and inertia. The 16 bit resolver-to-digital converter was then used to measure the angular speed of the aircraft in yaw. This tachometer has a scale factor of $2.27 \cdot 10^{-3} \text{ V/}^\circ/\text{s}$, a scale factor error of 10% and a bandwidth of 125Hz. The model $G(s)$ of the aircraft obtained from its step response is as follows :

$$G(s) = \frac{\dot{\theta}_a}{U_d} = \frac{2700}{(0.026s^2 + 0.232s + 1)},$$

where $\dot{\theta}_a$ is the angular speed ($^\circ/\text{s}$) of the aircraft and U_d is in Volts.

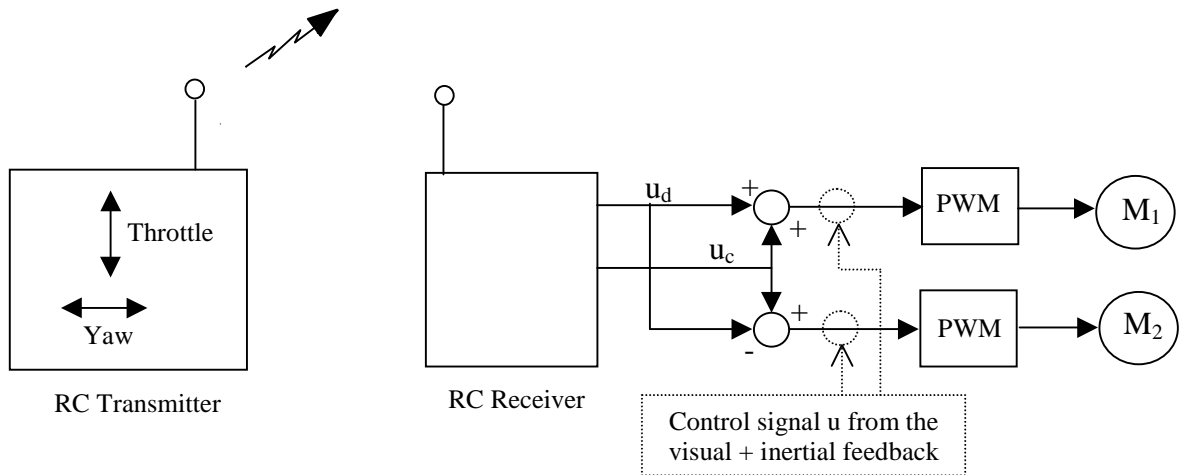


Fig. 7 Block diagram of the differential system driving the propellers

5.2. The visual inertial feedback system

The complete position feedback system we have designed is shown in Figure 8.

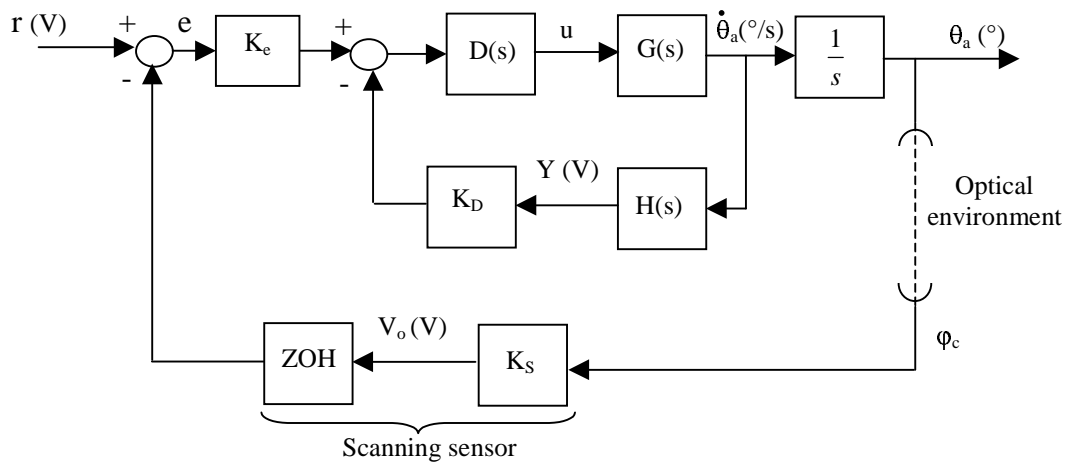


Fig. 8 Block diagram of the closed-loop visual control system incorporating the scanning visual sensor (outer loop) and a gyroscope (inner loop).

The scanning sensor is modelled by a simple gain $K_s \cong 1\text{V/}^\circ$ (cf Figure 5), and its output signal was maintained by a zero-order hold until the completion of each scan ($T = 100\text{ms}$). Since the transfer function from the controlling yaw input to the

yaw angle has three main poles, we incorporated a velocity feedback¹² using a miniature piezo gyroscope. The latter was modelled by the following transfer function $H(s)$:

$$H(s) = \frac{Y}{\theta_a} = \frac{6.7 \cdot 10^{-3}}{(0.0032s + 1)}$$

The gain $K_D = 5$ was chosen so as to give a closed loop step response with a settling time of 100ms with a minor overshoot. The controller $D(s)$ was designed in particular to compensate for the limited bandwidth (50Hz) of the gyroscope. $D(s)$ raised the phase margin further, compensating for the phase lag introduced by the low-pass filter $H(s)$, and thus increasing the damping. The transfer function of $D(s)$ is given by :

$$D(s) = 0.3 \left(\frac{0.08s + 1}{0.014s + 1} \right),$$

$$\text{and } K_e = 6 \cdot 10^{-2}$$

The frequency response of the open-loop transfer $B_o(s) = \frac{V_o(s)}{r(s)}$ is shown in Figure 9.

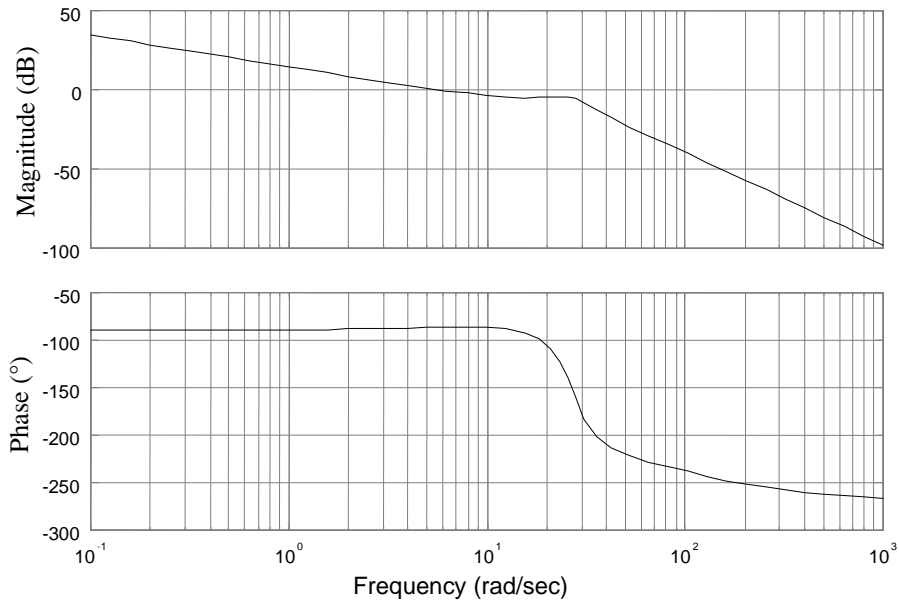


Fig. 9 Frequency response of $B_o(s)$

5.3. Target tracking and visual fixation

We assessed the closed-loop performance of the visual-inertial feedback system on the testbed described in Figure 6. Both the angular position of the dark edge (input) and the angular orientation in yaw of the model aircraft (output) were measured with potentiometers, as depicted in Figure 6.

Figure 10 illustrates the tracking performance of the visual feedback loop with respect to a sinusoidal variation of the position of a dark edge in the visual field of the scanning sensor. The response was found to lag behind the command by about 100 ms, i.e., by hardly more than the scan period, which turned out to be the main limiting factor. The maximum linear speed of the dark edge which the model aircraft was able to track was about 25 cm/s at a distance of 1m (14°/s). The

histogram in figure 11 shows that the aircraft steadily controls its two propellers so as to gaze steadily on a stationary target during a long 17 min experiment.

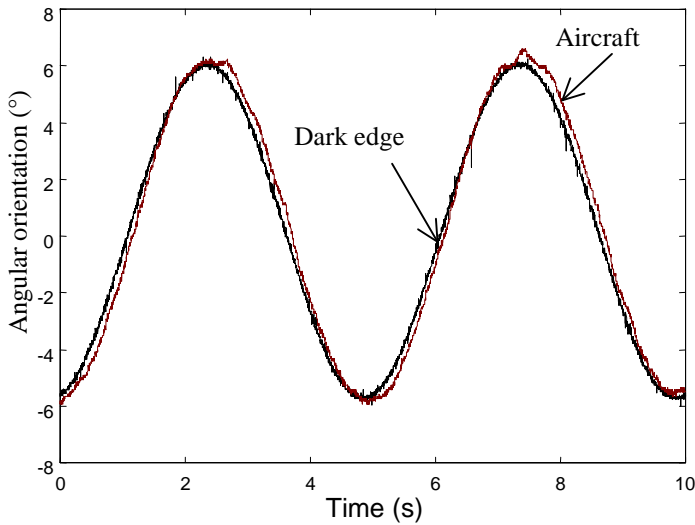


Fig.10 Dynamic performance of the overall twin-propeller system (cf Fig. 6) tracking a dark edge (contrast $m=0.2$) located at a distance of 1 m in front of the eye and oscillating at 0.2 Hz perpendicularly to its line of sight. $r = 5.5V$.

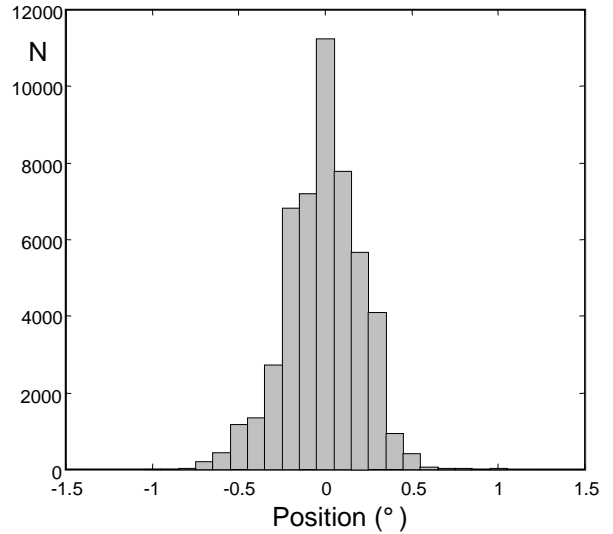


Fig. 11 Distribution of the angular orientation of the model aircraft, which constantly fixated a stationary dark edge ($m=0.2$) for 17 minutes. Number of samples = 50000 Acquisition time = 1000s Standard deviation = 0.22° .

6. CONCLUSION

In this paper, we describe the use of a low-level, low complexity, power-lean miniature sensor designed to provide a micro-air vehicle with visual stabilization and tracking possibilities. We established that a 100 gramme twin-propeller aircraft equipped with this miniature scanning eye can track an object with various levels of contrast (down to 10%) at various distances (up to 1.5 m), using its onboard electronics and energy in a completely autonomous manner.

The aim here was not to achieve a high performance closed-loop system such as those based on a CCD camera which recognize and track a target at high speeds. Such systems rely on more complex control laws and required larger computational resources.^{11,13} Our low-level visual system is not based on any “understanding of the environment”, and consequently cannot detect and track a specific target among many others. Yet this moderately complex, inexpensive (\cong 400 USD) system can be used:

- to stabilize a micro air vehicle around a given axis of rotation, where the time-constant is small (the small time-constants of micro air vehicles make it difficult for them to be stabilized by a human operator).
- to replace a gyroscope by maintaining an angular position with respect to environmental features, for a long time and with no drift.
- to track a target visually with a large shape, contrast and distance invariance, using a single pair of photosensors scanning concomitantly.

It is worth noting that the optical position-servoing method we have developed is based on a *position sensor* that relies on a *motion detector*. An essential message of this paper is that a simple, low amplitude scanning of two photoreceptors can provide positional information far beyond that expected from their angular sampling basis. Extending these results to a 1D or 2D photoreceptor array will retain this interesting property while enlarging the field of view.

ACKNOWLEDGMENTS

We thank M. Boyron for his expert technical assistance and I. Daveniere and J. Blanc for improving the English manuscript. This research was supported by CNRS (Life Sciences, Engineering Sciences, and Programme on Microsystems). S. Viollet received a predoctoral fellowship from Ministry of National Education and Scientific Research (MENRS).

REFERENCES

1. JM. Pichon, C. Blanes, and N. Franceschini, "Visual guidance of a mobile robot equipped with a network of self-motion sensors," in *Mobile Robots* **4**, pp. 44-53, SPIE, Bellingham (USA), 1989.
2. N. Franceschini, J. M. Pichon, and C. Blanes, "From insect vision to robot vision," *Phil Trans Roy Soc Lond B* **337**, pp. 283-294, 1992.
3. F. Mura, and N. Franceschini, "Visual control of altitude and speed in a flying agent," in *Proc From Animals to Animats*, pp. 91-99, eds. Cliff and Husbands, Cambridge, 1994.
4. F. Mura, and N. Franceschini, "Biologically inspired Retinal Scanning enhances motion perception of a mobile robot," *Proc 1st Europe-Asia Congress on Mechatronics* **3**, pp. 934-940, ed. A. Bourjault, Besançon, 1996.
5. S. Viollet, and N. Franceschini, "Biologically-Inspired Visual Scanning Sensor for Stabilization and Tracking," in *Proc IEEE IROS'99* **1**, Kyongju (Korea), pp. 204-209, 1999.
6. N. Franceschini, and R. Chagneux, "Repetitive scanning in the fly compound eye," in *Proc Göttingen Neurobiology Conf*, eds. Wässle and Elsner, 1997.
7. F. Mura, and I. Shimoyama, "Visual Guidance of a Small Mobile Robot Using Active, Biologically-Inspired, Eye Movements," in *Proc IEEE Robotics and Automation*, pp. 1859-1864, Leuven, 1998.
8. N. Franceschini, A. Riehle, and A. Le Nestour, "Directionally Selective Motion Detection by Insect Neurons," *Facets of Vision*, pp. 360-390, eds. Stavenga & Hardie, Springer, Berlin, 1989.
9. R. C. Hardie, "Functional organisation of fly retina," *Progress in Sensory Physiology* **5**, pp. 1-79, ed. D. Ottoson, Springer, Berlin, 1985.
10. N. Franceschini, C. Blanes, and L. Oufar, "Appareil de mesure passif et sans contact de la vitesse d'un objet quelconque," *Dossier Technique ANVAR/DVAR N° 51 549*, Paris, 1986.
11. P. I. Corke, "Dynamic Issues in Robot Visual-Servo Systems," *Robotics Research*, pp. 488-498, eds. Girald and Hirzinger, Springer, Berlin, 1996.
12. G. F. Franklin, J. D. Powell, and A. Emami-Naeini, *Feedback Control of Dynamic Systems*, Addison Wesley, 1994.
13. I. Ishii, Y. Yoshihiro, and M. Ishikawa, "Target Tracking Algorithm for 1ms Visual Feedback System Using Massively Parallel Processing," in *Proc IEEE Robotics and Automation*, pp. 2309-2314, Mineapolis, 1996.